

**EFFICIENT TREATMENT OF 3D TIME-DOMAIN  
ELECTROMAGNETIC SCATTERING SCENES BY  
DISJOINTING SUB-DOMAINS AND WITH  
CONSISTENT APPROXIMATIONS**

**V. Mouysset**

Laboratory MIP  
University Paul Sabatier  
31062 Toulouse Cedex 9, France

**P. A. Mazet**

Department of Informatic Treatment and Modelization  
ONERA Toulouse  
2 Avenue Edouard Belin, 31055 Toulouse Cedex, France

**P. Borderies**

Department of ElectroMagnetism and Radar  
ONERA Toulouse  
2 Avenue Edouard Belin, 31055 Toulouse Cedex, France

**Abstract**—Aim of this paper is to present an efficient scheme of domain decomposition to study, in the time domain, multiple scattering by separated obstacles and sources with any composition and geometry, in an homogeneous media. A method of decomposition into disjointed sub-domains is proposed, resting onto an homogeneous and adaptable approximation of coupling terms and leading to a natural parallelized and hybrid numerical schema. It permits to significantly lower the cumulative error of dissipation and/or dispersion introduced by classical scheme. It also leads to a suitable answer for a wide class of problems involving large scattering scenes limiting for classical time domain methods. Numerical examples are given to illustrate it.

## 1. INTRODUCTION

This paper is devoted to the research of a pertinent numerical approach to handle large electromagnetic scattering scenes in time domain. Unfortunately, straightforward answers are no longer suitable in this case. As an example, it is well-known that for the introduction of the Finite Difference in Time Domain (FDTD) method [21], numerical calculus to solve electromagnetic problems has been improved. However, this method, like the others, induces errors on the solution. They are dispersive ones. If this scheme can give fast and low storage accurate results in most of the cases, treatment of wide scattering scenes is still a delicate problem. Indeed, as the global volume of the mesh grows, dispersive errors are cumulated and increase. Hence, when being interested in the simulation of coupling between some disjointed elements and sources, these cumulative errors lead to an obviously divergent solution.

An answer to this problem can be found in a refinement of the global mesh. Another one could rest onto hybridization between several different schemes like FDTD, Finite Volume (FVTD) and Time Integrated Methods (TIM) [15]. Nevertheless, none of them are suitable in regard of the overall cost (in terms of memory and CPU time) to perform the computation of a large scene [10, 16, 19].

A restrictive point to these approaches lies into the necessity to mesh the free space between the obstacles/sources. Indeed, a local refinement does not ensure a gain of accuracy on the whole solution, so free space parts have to be refined too. *A contrario*, when computing by TIM, no useless volumes are introduced. Hence a natural idea is to isolate all obstacles and sources into disjointed sub-domains (when they are not too close one each other) and “forget” the free space part. Coupling between all the sub-domains will therefore be evaluated by use of an integral formula.

Main difficulties of this approach can be summed up into two steps: the *anterpolation* and the *interpolation* phases. This terminology comes from the Fast Multipole Method (FMM) used to solve integral equations in the frequency domain (see [4] and references). The first phase consists in evaluating contributions from one domain to the others. The second step is to interpolate computed fields during the anterpolation and update contributions onto a given domain from the other ones.

One way to treat this multi-domain approach, introduced by Olivier [14] and later extended by Johnson and Rahmat-Samii [5], lays onto restriction of computational domains by Absorbing Boundary Conditions (ABC) derived from integral representation of the

electromagnetic fields. EM-fields are then evaluated using FDTD and coupling between domains, by the time-domain equivalence principle, can then be done by some Kirchhoff's formula. However the authors notice problems of stability, consistency and very significant over-costs in their numerical experiments. To improve the method and make it suitable, Bernardi *et al.* [2] tried to lower costs of the antepolation stage, basically by introducing small groupings onto the surfaces used to apply the equivalence principle. From another point of view, Xu and Hong recently derived a specific integral formula in the 2D case to make the interpolation stage cheaper [20]. However, stability and consistency problems are still noticed. At last, a significant gain on the global cost of the method could rest on "compressive" algorithms such as the one introduced to treat the ABC in [7].

In this paper we are going to present another way to solve the multi-domain problem. The first crucial point lays onto its formulation as a system of sub-problems of Maxwell's equations where each one is homogeneous out of a given volume. Coupling terms will be given as currents on Huygens' surfaces and evaluated by some specific integral formula. Main differences between our method and previous ones can be summed into three specific elements.

First, the decomposition we are going to detail in the sequel could appear as being very similar as [14, 5]. Nevertheless, we propose a different starting point by expressing the coupled system of Maxwell's equations as the search for  $n$  electromagnetic fields  $(E^i, H^i), i = 1 \dots n$ , where previously only one  $(E, H)$  was looked for. In this second case, the only ABC which can be used is given by Dirichlet-to-Neumann or Neumann-to-Dirichlet operators, On-Surface Radiating Conditions (OSRC) or Integral Radiating Boundary Conditions (IRBC) for example. Main advantage of this new decomposition is then to solve small Maxwell's systems in homogeneous media whose can be bounded using any ABC and replace OSRC or IRBC by Perfectly Matched Layers (PML) for example.

Then, efficiency for the antepolation stage arises from a fast and accurate approximation of any given integral representation of electromagnetic fields propagating into the vacuum. This is a crucial point to simplify expression of these non-local expressions. A classical one is the well known Far Field formula [22]. It provides fast computations and good results. However, as its accuracy is quantified in  $O(1/d)$  ( $d$  being the distance from the surface were electromagnetic currents are taken to the observatory), in the context of a given scattering scene we can not ensure  $1/d$  to be neglectible in regard of all errors introduced by used scheme. It can be enforced by developing to various higher orders of  $1/d$  as done for the Near-to-Near formulas

(see [3, 6, 17, 18]). Again, computations of these methods either have a too restrictive range of applications, or present a significant over-cost according to the performances we are looking for. Our previous work [11, 13] was dedicated to establish and study another radiation formula, called Near-to-Relative-Far. Its error is given in terms of  $\delta/d$ , where  $\delta$  stands for an adaptive and local parameter. In the present paper, we will chose to consider this formula to compute the coupling terms. Consequently we will be able to present a balanced system between accuracy and performances.

At last, for the interpolation phase, the steady point is to diminish the number of values necessary to reconstruct the contributions into any given sub-domain from all the others. A straightforward summation of these contributions onto the full discretization of a Huygens surface is not realistic due to the amount of data involved. Our approach is to introduce again an approximation in  $\delta/d$  which considerably reduce the numerical effort. Once again, we will be able to take the tradeoff between efficiency and numerical errors.

Hence, in this paper we will successively derive the method (Section 2). Then we will present some numerical experiments to highlight its efficiency (Section 3), before concluding (Section 4).

## 2. MULTI-DOMAIN DECOMPOSITION

Consider the coupling problem composed of sources and scatterers spread over an homogeneous medium. Principle of the method is to separate each element (source or scatterer) from the others into disjointed domains  $\mathcal{D}^i, i = 1..n$ . Then we *pick up* electric and magnetic currents,  $J^i = \mathbf{n}_{\mathcal{P}^i} \times H$  and  $M^i = -\mathbf{n}_{\mathcal{P}^i} \times E$ , onto polyhedral surfaces (even not convex ones)  $\mathcal{P}^i$ , so-called *pick up surfaces*. From these  $J^i$  and  $M^i$  we evaluate contributions from a given domain  $\mathcal{D}^i$  to the others, and introduce them as source terms onto Huygens surfaces noted  $\mathcal{H}^i, i = 1..n$ . See Figure 1 for an illustration of this principle. Non local sources (like plane waves) will be taken into account by introducing them onto the Huygens surfaces.

We want to determine electromagnetic field versus time at given points in the outer space of each domain, and (possibly) other ones into the domain close to the obstacle/source.

### 2.1. Formulation of the Problem

For the sake of simplicity in reading whole equations, let us introduce the following notations:

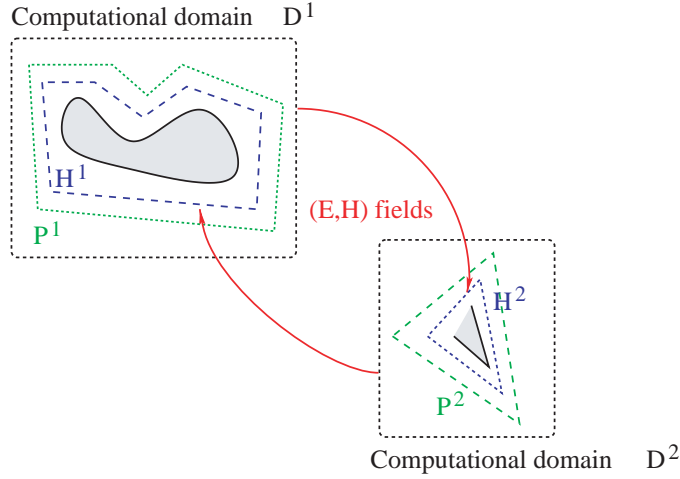


**Figure 1.** Principle of the multi-domain decomposition.

- let  $u = (E, H)^T$  be the electromagnetic field, and  $u^{inc} = (E^{inc}, H^{inc})^T$  be the exterior source terms,
- for any given index  $i$ ,  $i^*$  will stand for any index  $j$  such that  $j \neq i$ , consequently  $\sum_{i^*} A_{i^*}$  will stand for  $\sum_{j \neq i} A_j$ ,
- to any given surface  $\mathcal{F}$  we associate as  $V(\mathcal{F})$  the embedded volume by  $\mathcal{F}$ , and  $\mathbf{n}_{\mathcal{F}}$  its outward unitary normal vector,
- to any given Huygens surface  $\mathcal{H}^i$ , we introduce the tangential operator

$$B_i^{\mathcal{H}} = \begin{pmatrix} 0 & \mathbf{n}_{\mathcal{H}^i} \times \delta_{\mathcal{H}^i} \\ -\mathbf{n}_{\mathcal{H}^i} \times \delta_{\mathcal{H}^i} & 0 \end{pmatrix},$$

- and, at last, to any given pick-up surface  $\mathcal{P}^i$ , the following tangential operator  $B_i^{\mathcal{P}}$  will be defined  $B_i^{\mathcal{P}} =$
- $$\begin{pmatrix} 0 & \mathbf{n}_{\mathcal{P}^i} \times \delta_{\mathcal{P}^i} \\ -\mathbf{n}_{\mathcal{P}^i} \times \delta_{\mathcal{P}^i} & 0 \end{pmatrix}.$$

Using these notations, the whole scattering problem we have to solve is given by instationnary Maxwell equations:

$$\begin{cases} \mathbb{A}(x) \partial_t u + \mathbb{R}u + \mathbb{B}(x)u = u^{inc}, \\ u(t=0) = 0, \end{cases} \quad (1)$$

where

$$\mathbb{A}(x) = \sum_i \begin{pmatrix} \varepsilon_r^i(x) \varepsilon_0 \mathbb{I}_3 & 0 \\ 0 & \mu_r^i(x) \mu_0 \mathbb{I}_3 \end{pmatrix} = \sum_i \mathbb{A}_i(x),$$

$$\mathbb{R} = \begin{pmatrix} 0 & -\nabla \times \\ \nabla \times & 0 \end{pmatrix}, \text{ and } \mathbb{B}(x) = \sum_i \mathbb{B}_i(x).$$

Each operator of multiplication  $\mathbb{B}_i(x)$  is supposed to be non-negative and localized into its corresponding domain  $\mathcal{D}^i$ . Each of them represents the dissipative comportment of sources/obstacles enclosed into  $\mathcal{D}^i$  (e.g., conductivity terms). By the same way,  $\mathbb{A}_i(x)$  represents the electric and magnetic characteristic of sources/obstacle in  $\mathcal{D}^i$ . At last,  $u^{inc}$  are electric and magnetic sources. This includes in the same time sources embedded in the domains (e.g., antennas, source points), and exterior ones (e.g., plane waves) which can be introduced onto the Huygens surfaces surrounding obstacles/sources into  $\mathcal{D}^i$ .

Thus, let us introduce  $G$  the Green kernel of homogeneous unstationary Maxwell's equations, and denote by  $f *_{(t,X)} g$  the space-time convolution of functions  $f$  and  $g$ , and  $Y_W$  is the characteristic function on any given space domain  $W$ .

Then the multi-domain principle can be expressed as:

$$\begin{cases} \text{Find } u_i, i = 1..n \text{ solutions to} \\ \mathbb{A}_i(x) \partial_t u_i + \mathbb{R} u_i + \mathbb{B}(x) u_i = u^{inc} Y_{\mathcal{D}^i} \\ + B_i^{\mathcal{H}} \left( \sum_{i^*} G *_{(t,X)} B_{i^*}^{\mathcal{P}} u_{i^*} \right), \\ u_i(t=0) = 0. \end{cases} \quad (2)$$

Then, instead of looking for the solution of the large problem (1) involving multiple scatterers/sources spread over the whole space, we are led to solve  $n$  *local scattering problems* of kind (2) with coupling terms given as source terms on each problem by  $B_i^{\mathcal{H}} \left( \sum_{i^*} G *_{(t,X)} B_{i^*}^{\mathcal{P}} u_{i^*} \right)$ .

## 2.2. Link between Problems (1) and (2)

As we will search all the functions  $u_i, i = 1..n$  instead of  $u$  because they can be defined (in a domain smaller than the whole problem one), they appear as a kind of *partial solutions*. Obviously, according to the decomposition we suggest in the beginning of this section, it appears that solutions  $u$  to system (1), and  $(u_i)_{i=1..n}$  to (2), verify the following relations:

- for the *interior* part of the problem:  $\forall i, \forall (t, X) \in \mathbb{R}^+ \times V(\mathcal{H}_i)$

$$u(t, X) = u_i(t, X), \quad (3)$$

- and for the *exterior* part:  $\forall(t, X) \in \mathbb{R}^+ \times (\cup_i \mathcal{D}_i)^c$

$$u(t, X) = \sum_i G^{*(t, X)} B_i^{\mathcal{P}} u_i. \quad (4)$$

This can be easily seen by considering the following function  $\tilde{u}$

$$\tilde{u} = \sum_i \left[ Y_{\mathcal{D}^i} u_i + \prod_{i^*} Y_{V(\mathcal{H}^{i^*})^c} Y_{(\mathcal{D}^i)^c} G^{*(t, X)} B_i^{\mathcal{P}} u_i \right]. \quad (5)$$

Indeed, by reporting  $\tilde{u}$  in (1) and evaluating it first in each domain  $\mathcal{D}^i$ , and then in the exterior space of  $\cup_i \mathcal{D}^i$ , we verify that  $\tilde{u}$  is solution of (1) onto the whole domain  $\mathbb{R}^+ \times \mathbb{R}^3$ , and so  $\tilde{u} = u$ . Hence, restricting (5) to any  $V(\mathcal{H}_i)$  leads to (3). By the same way, its restriction to  $(\cup_i \mathcal{D}_i)^c$  gives (4).

Then, using equation (3) we have the value of electromagnetic field inside each volume  $V(\mathcal{H}_i)$  simply by the solution (2) in this volume ; and using equation (4) we will be able to compute the electromagnetic field in the exterior domain  $(\cup \mathcal{D}^i)^c$ .

We can notice that according to previous relations (3) and (4), solving (2) involves only  $u_i$  values in domain  $\mathcal{D}^i$ . So, significant profit of the multi-domain method lies into the possibility of restricting computational domains for all  $u_i$  to their own domain  $\mathcal{D}^i$  by use of Absorbing Boundary Conditions like Perfectly Matched Layers (PML) [1]. This is a keypoint of the method which leads to a set of small and realistic computational problems.

### 2.3. Anterpolation-interpolation Principle

Main problem solving (2) and using formula (4) is the non-local character of the space-time convolution by Green's kernel  $G$ . Practically it involves huge data storage and strong computations to have a fine result. In the frequency domain, these are well-known difficulties in programming Integral Equations to solve Maxwell's equations. Hence, we will propose to follow a similar way as used in the Fast Multipole Methods (see [4] and references) by introducing two phases in the solving process:

- (i) an *anterpolation* phase which consists in computing the contribution from a given domain  $\mathcal{D}^i$  to the others,
- (ii) an *interpolation* phase which is the reconstruction of the coupled problem by adding all contributions coming from the other domains  $\mathcal{D}^{i^*}$ .

Moreover, in each of these two phases, approximations are introduced in order to simplify calculations and to diminish storage and CPU time costs.

### 2.3.1. Anterpolation

According to system (2), anterpolation lies onto the calculus of the coupling term  $G^{*(t,X)} B_i^{\mathcal{P}} u_i$ , from solution  $u_i$  of (2) on domain  $\mathcal{D}^i$ , to each point of the Huygens' surface  $\mathcal{H}^{i*}$  in any other domain  $\mathcal{D}^{i*}$ . As  $G^{*(t,X)} B_i^{\mathcal{P}} u_i$  is computed from currents on the pick-up surface  $\mathcal{P}^i$  to points in the outer domain of  $V(\mathcal{P}^i)$ , according to the sub-domain splitting made in the first section, we can ensure that the distance from such a point  $X$  to this surface  $\mathcal{P}^i$  is strictly greater than a minimal distance  $d > 0$ . As it is, we will use the *Near-To-Relative-Far* (NTRF) radiation method introduced in [11] to compute  $(E_i, H_i)$  values at point  $X$ :

$$\begin{aligned} E_i(t, X) \approx & \sum_k \int_{\mathcal{P}_k^i} \left[ \frac{1}{c_0 d_k} (Z_0 \mathbf{T}_k \partial_t J_i - \mathbf{t}_k \times \partial_t M_i) \right. \\ & + \frac{Z_0}{d_k^2} \left( 3\mathbf{T}_k J_i - 2\mathbf{N}_k J_i - \frac{1}{Z_0} \mathbf{t}_k \times M_k \right) \\ & \left. + \frac{c_0 Z_0}{d_k^3} \int_t (3\mathbf{T}_k J_i - 2\mathbf{N}_k J_i) \right] (t - T_k, y) \frac{dy}{4\pi}, \end{aligned} \quad (6)$$

$$\begin{aligned} H_i(t, X) \approx & \sum_k \int_{\mathcal{P}_k^i} \left[ \frac{1}{c_0 d_k} \left( \frac{1}{Z_0} \mathbf{T}_k \partial_t M_i + \mathbf{t}_k \times \partial_t J_i \right) \right. \\ & + \frac{1}{Z_0 d_k^2} (3\mathbf{T}_k M_i - 2\mathbf{N}_k M_i + Z_0 \mathbf{t}_k \times J_i) \\ & \left. + \frac{c_0}{Z_0 d_k^3} \int_t (3\mathbf{T}_k M_i - 2\mathbf{N}_k M_i) \right] (t - T_k, y) \frac{dy}{4\pi}, \end{aligned} \quad (7)$$

where  $\mathbf{T}_k v = \mathbf{t}_k \times (\mathbf{t}_k \times v)$ ,  $\mathbf{N}_k v = \mathbf{n}_k \times (\mathbf{n}_k \times v)$ ,  $Z_0 = \sqrt{\frac{\mu_0}{\varepsilon_0}}$  and  $c_0 = \frac{1}{\sqrt{\mu_0 \varepsilon_0}}$ ;  $T_k = d_k/c_0$  stands for the time for the signal to travel from  $X_k$  to point  $X$ . Formulas (6-7) are constructed with an arbitrary cutting out of  $\mathcal{P}^i$  into a set of small "sub-faces"  $(\mathcal{P}_k^i)_k$ , and choosing points  $X_k \in \mathcal{P}_k^i$ . At last,  $\mathbf{n}_k$  is the outward unitary normal vector to  $\mathcal{P}_k^i$ , and  $\mathbf{t}_k$  is the normalized vector  $\mathbf{t}_k = \frac{1}{d_k} \overrightarrow{X X_k}$ .

These approximations are established under the following

assumption (see [11, 13])

$$d^{-1}\delta \ll 1, \quad (8)$$

where  $\delta$  is a characteristic length describing a reference sub-face  $\mathcal{S}$  ( $\mathcal{S} = C\delta^2$  with  $C > 0$ ) such that each sub-face of  $\mathcal{P}^i$  is smaller than  $\mathcal{S}$ ; and  $d$  stands for the smallest value of all  $d_k, k$ .

Hence, we can sum up the anterpolation phase by the following approximation

$$G^{*(t,X)} B_i^{\mathcal{P}} u_i \approx [\widetilde{G^{*(t,X)}}] B_i^{\mathcal{P}} u_i, \quad (9)$$

where  $[\widetilde{G^{*(t,X)}}] B_i^{\mathcal{P}} u_i$  stands for the value of  $(E_i, H_i)$  computed at  $X$  using formulas (6) and (7).

Main interests in using the Near-to-Relative Far formula for the anterpolation phase are lying into the following considerations:

- (i) First terms of formula (6)–(7) (terms in  $d^{-1}$ ) can be interpreted as a time-localized version of Yee's far field expression [22]. As other terms are decreasing faster when  $d$  grows (in  $d^{-2}$  and  $d^{-3}$ ), this ensures us to have same fine results as using Yee's far field. This point validates straightforwardly the far field behavior of our formulations. Moreover, numerical experiments are also validating the accuracy of the NTRF formula when observation point  $X$  is coming very close to the pick-up surface (at a few cells from  $\mathcal{P}^i$ ).
- (ii) As higher order terms (in  $d^{-2}$  and  $d^{-3}$ ) have basically the same expression as lower ones (in  $d^{-1}$ ), numerical implementation of (6-7) will not be more complicated than the well-known Yee's far field implementation [8].
- (iii) Error introduced by derivations leading to formulas (6)–(7) is given in  $O(\sup_i ((d_i)^{-1}\delta_i))$ . To grant the error to be small with this estimation leads to consider the following alternative:
  - consider that  $X$  is far from every  $\mathcal{P}_k^i$  ( $d \rightarrow \infty$ ),
  - or give a finer set of  $\mathcal{P}_i$  if  $X$  is closer ( $\delta \rightarrow 0$ ).

This explains the *Relative-Far* character of formulas (6)–(7). Distance  $d$  to the observation point is no longer an absolute and unique criterion like for Near-to-Far or Near-to-Near formulas. This is now its comparison with a sizable characteristic edge  $\delta$  of the sub-faces splitting  $(\mathcal{P}_k^i)_k$  which is considered.

### 2.3.2. Interpolation

The other restrictive point, on a computational point of view, lies onto the necessity to have  $u_{i*}$  values onto the whole Huygens surface  $\mathcal{H}^i$ .

This involves an *a priori* huge number of points onto  $\mathcal{H}^i$  to give an accurate result. But the more numerous sampling points are, the more expensive computations will be. Aim of the *interpolation* phase is to restrict this number of points to a lower one, and to give a method of reconstruction to evaluate  $u_{i*}$  values onto the whole  $\mathcal{H}^i$  with only these few points.

To do so, we consider two points  $X$  and  $X'$ , and we evaluate electromagnetic fields by (6)–(7). They will be respectively referred to as  $(\tilde{E}, \tilde{H})$  and  $(\tilde{E}', \tilde{H}')$ . We also denote by  $d_k$  and  $d'_k$  the two distances  $d_k = |X_k - X|$  and  $d'_k = |X_k - X'|$ , and by  $\mathbf{t}_k$  and  $\mathbf{t}'_k$  the two normalized vectors  $\mathbf{t}_k = \frac{1}{d_k} \overrightarrow{X X_k}$  and  $\mathbf{t}'_k = \frac{1}{d'_k} \overrightarrow{X' X_k}$ .

As it was done for the Huygens surfaces by introducing a cutting out of characteristic length lower than  $\delta$ , we assume symmetrically that  $|X - X'| \leq \delta$ . Following inequalities take place

$$d_k - \delta \leq d'_k = \left| \overrightarrow{X' X} + \overrightarrow{X X_k} \right| \leq \delta + d_k, \quad (10)$$

and under the assumption  $\delta d_k^{-1} \ll 1$  we have

$$\begin{aligned} |\mathbf{t}_i - \mathbf{t}'_i| &= \frac{1}{d_i} \left| \frac{d_i}{d'_i} \overrightarrow{X'_0 X_i} - \overrightarrow{X_0 X_i} \right| \\ &= \frac{1}{d_i} \left| \frac{d_i - d'_i}{d'_i} \overrightarrow{X_0 X_i} - \frac{d_i}{d'_i} \overrightarrow{X'_0 X_0} \right| \\ &\leq \frac{1}{d_i} \left( \frac{\delta}{d'_i} d_i + \frac{d_i}{d'_i} \delta \right) = O\left(\frac{\delta}{d_i}\right). \end{aligned} \quad (11)$$

Then we evaluate  $\left| (\tilde{E}, \tilde{H})^T - (\tilde{E}', \tilde{H}')^T \right|$  using (6-7) and we introduce the inequalities (10)–(11). This leads to (see [12] for the complete details of the proof)

$$\left| \begin{pmatrix} \tilde{E} \\ \tilde{H} \end{pmatrix} - \begin{pmatrix} \tilde{E}' \\ \tilde{H}' \end{pmatrix} \right| \leq O\left(\frac{\delta}{d}\right), \quad (12)$$

where  $d$  is such that on each  $\mathcal{P}^i$  we have  $0 < d \leq d_k, \forall k$ .

Hence, relation (12) ensures that for any given point  $X$ , and any  $X'$  such that  $|X - X'| \leq \delta$ , the difference between the values of electromagnetic fields computed by (6-7) at  $X$  and  $X'$  has the same order as the error made when computing them (i.e. in  $O(\delta/d)$ ).

So, *interpolation* phase consists simply in computing  $u_i$  values at some reference points of the Huygens surface  $\mathcal{H}^i$  and to assume it to

have the same value at neighboring points (situated at less than  $\delta$  from the reference ones). This can be summed up by the approximation

$$B_i^{\mathcal{H}} \approx [\widetilde{B_i^{\mathcal{H}}}], \quad (13)$$

where  $[\widetilde{B_i^{\mathcal{H}}}]$  stands for the piecewise function previously introduced.

### 2.3.3. Full Scheme of the Multi-domain Method

According to (9) and (13), the multi-domain method can be summed up as the following approximation of (2):

$$\text{Find } \tilde{u}_i, i = 1..n \text{ solutions to } \begin{cases} \mathbb{A}_i(x)\partial_t \tilde{u}_i + \mathbb{R}\tilde{u}_i + \mathbb{B}(x)\tilde{u}_i = \\ [\widetilde{B_i^{\mathcal{H}}}] \left( u^{inc} + \sum_{i^*} [\widetilde{G^*(t,X)}] B_{i^*}^{\mathcal{P}} \tilde{u}_{i^*} \right), \\ \tilde{u}_i(t=0) = 0, \end{cases} \quad (14)$$

where  $[\widetilde{B_i^{\mathcal{H}}}]$  and  $[\widetilde{G^*(t,X)}] B_{i^*}^{\mathcal{P}} \tilde{u}_{i^*}$  are respectively defined by (13) and (9), and  $\tilde{u}_i$  stands for the approximation of  $u_i$ .

Moreover, when functions  $u_i$  are smooth enough, we can ensure that error done in solving (14) instead of (2) is given by

$$\|u_i - \tilde{u}_i\| \leq O\left(\frac{\delta}{d}\right). \quad (15)$$

Stability in finite time of the full system (14) is proved in [12].

## 3. NUMERICAL EXAMPLE: COUPLING BETWEEN AN ANTENNA AND A VEHICLE

We look at the coupling problem between a car (only the metallic parts are considered) and a given antenna. As the antenna is located at two meters away from the car, we perform a decomposition in sub-domain as represented on Figures 2–3. The antenna is assumed to be the only source of this case, and coupling effects are naturally taken into account by the two different approaches tested there: a single domain decomposition using a FDTD method, and the multi-domain decomposition by the multi-domain method. Its bandwidth is from 20 MHz to 1 GHz. Smallest mesh size on each domain is above  $h = 0.0125$  m, and time step used is of  $2.5 \cdot 10^{-11}$  s. Moreover, costs in term of CPU time and memory are detailed in the Table 1.

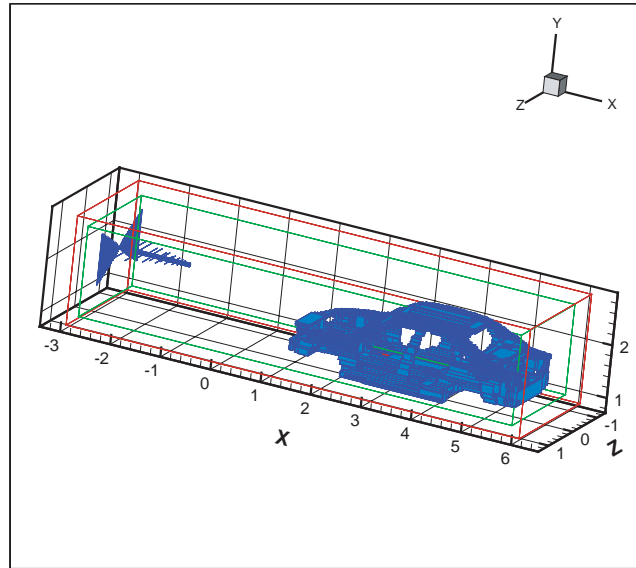


**Figure 2.** Computational domains for one domain and multi-domain methods: One domain configuration.

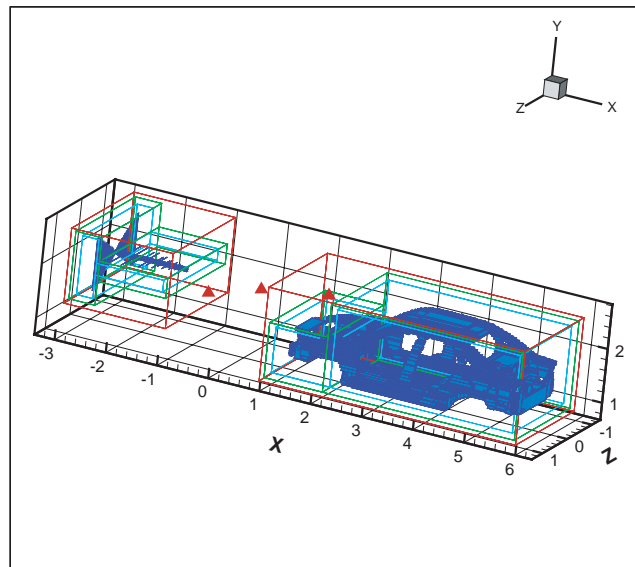


**Figure 3.** Computational domains for one domain and multi-domain methods: Multi-domain decomposition.

To perform the computations on the multi-domain case, we have chosen a  $\delta/d$  maximal value of 0.15 in the car sub-domain and also of 0.15 in the antenna one. This leads to the results presented in the Figures 4-5. The observation point ( $P_1$ ) is placed at half distance between the car and the antenna.

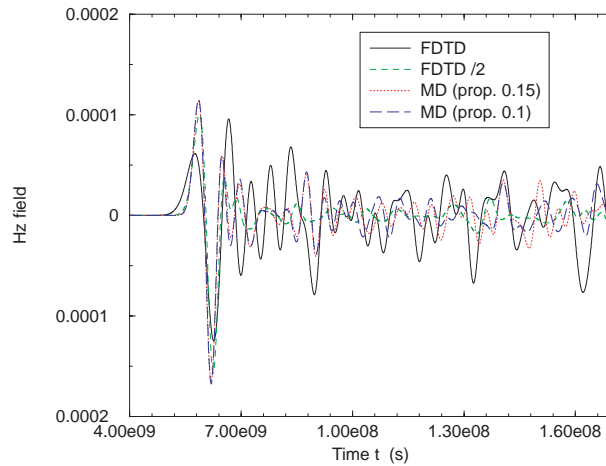


**Figure 4.** Comparison of results obtained respectively with one domain and multi-domain methods: Results at point  $P_1$ .

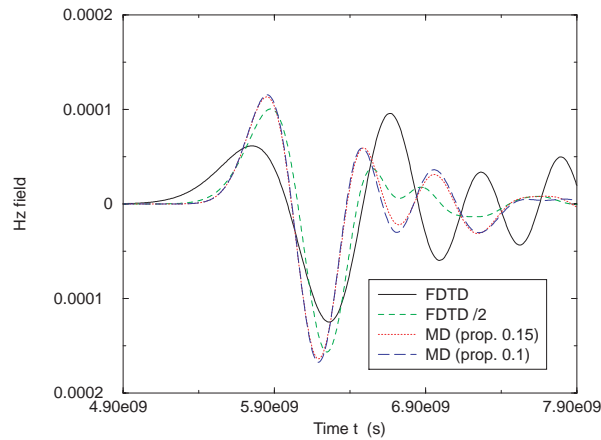


**Figure 5.** Comparison of results obtained respectively with one domain and multi-domain methods: Detail of the results at point  $P_1$ .

**Table 1.** Comparison of costs between domain and multi-domain computations (values are compared to the one domain FDTD results).

Method	CPU Time	Memory cost
One domain FDTD ( $h$ )	x1	x1
One domain FDTD ( $h/2$ )	x13.61	x6.36
MD (prop. 0.15) [antenna] ( $h$ )	x5.01	x0.29
MD (prop. 0.15) [car] ( $h$ )	x8.1	x0.62
MD (prop. 0.1) [antenna] ( $h$ )	x9.01	x0.32
MD (prop. 0.1) [car] ( $h$ )	x21.18	x0.66

We have performed the one domain computations onto two meshes: a  $h$  mesh and a  $h/2$  one. The multi-domain mesh is obtained as two parts (one around the antenna, and the other close to the car) of the mono-domain one in  $h$ . On Figure 4, one can see that results are roughly the same for all the methods. Moreover, we see that the multi-domain method is stable for long time computations.

The most important point is lying into the Figure 5 where one can see that a refinement of the meshing for one domain computations brings curves very close to the multi-domain ones. Indeed, the  $h$  computations for one domain calculus are suffering from the dispersive errors of the method cumulated from the antenna to the car. This is very easy to see when refining to a  $h/2$  mesh and comparing the curves. However, when using the multi-domain decomposition we have a very accurate result even if we use the coarse mesh. This is in agreement with the aim of the method which was to enforce the precision of the coupling by diminishing the cumulative errors due to dispersion onto wide meshes.

At last, if we compare the costs relative to each calculus (see table 1) we can see that for a equal or better accuracy on the solution, the multi-domain method involves less memory and requires almost the same time as for the fine one-domain computations. This makes our method a very interesting and efficient one to study this kind of configurations.

#### 4. CONCLUSION

In this article, we have presented a new decomposition into disjointed sub-domains for accurate and efficient computing of wide scattering scene in an homogeneous lossless media. It can give with the same accuracy values for the electromagnetic fields close to the

obstacles/sources (in the computational domains) and at almost any points in the media (out off the computational domains).

Accuracy of this method is linked to a free and homogeneous parameter  $\delta/d$  which can be set arbitrarily. It follows a consistent scheme where the free parameter  $\delta$  induces natural groupings onto Huygens and pickup surfaces which permits to relax significantly the computational effort. This provides a suitable numerical response for a large class of scattering problems, and an hybrid method easy to parallelize. Moreover, it has been successfully applied onto a realistic example.

At last, all these development are led in the time domain so wide-band and transient problems are naturally taken into account.

## ACKNOWLEDGMENT

The authors would like to thank the GEMCAR project to provide the mesh used in the example of scattering by a car (described on Figures 2–3).

## REFERENCES

1. Berenger, J. P., “Three-dimensional perfectly matched layer for the absorption of electromagnetic waves,” *Journal of Comp. Phy.*, Vol. 127, 363–379, 1996.
2. Bernardi, P., M. Cavagnaro, S. Pisa, and E. Piuze, “Evaluation of human exposure in the vicinity of a base-station antenna using the multiple-region/FDTD hybrid method,” *IEEE Microwave Symposium Digest*, 1747–1750, 2002.
3. Craddock, I. J. and C. J. Railton, “Application of the FDTD method and a full time-domain near-field transform to the problem of radiation from a PCB,” *Journal of Electromagnetic Waves and Applications*, Vol. 6, 5–18, 1992.
4. Darve, E., “Fast-multipole method: Numerical implementation,” *Journal of Comp. Phy.*, Vol. 160, 195–240, 2000.
5. Johnson, J. M. and Y. Rhamat-Samii, “MR/FDTD: a multiple-region finite-difference-time-domain method,” *Microwave and Optical Technology Letters*, Vol. 14, 101–105, 1997.
6. Kragalott, M., M. S. Kluskens, and W. P. Pala, “Time-domain fields exterior to a two-dimensional FDTD space,” *IEEE Trans. on Ant. and Prop.*, Vol. 45, 1655–1663, 1997.
7. Lu, M., M. Lv, A. A. Ergin, B. Shanker, and E. Michielssen, “Multilevel plane wave time domain-based global boundary kernels for

- two-dimensional finite difference time domain simulations,” *Radio Science*, Vol. 39, RS4007:1-16, 2004.
8. Luebbers, R. J., K. S. Kunz, M. Schneider, and F. Hunsberger, “A finite-difference time-domain near zone to far zone transformation,” *IEEE Trans. on Ant. and Prop.*, Vol. 39, 429–433, 1991.
  9. Martin, T., “An improved near to far zone transformation for the finite difference time domain method,” *IEEE Trans. on Ant. and Prop.*, Vol. 46, 1263–1271, 1998.
  10. Maystre, D., “Electromagnetic scattering by a set of objects: an integral method based on scattering properties,” *Progress In Electromagnetics Research*, PIER 57, 55–84, 2006.
  11. Mouysset, V., “On an approximation of propagated fields by unstationary Maxwell equations, homogeneous off a bounded domain,” *C. R. Acad. Sci. Ser. I*, Vol. 341, 641–646, 2005.
  12. Mouysset, V., “A sub-domain method to solve time domain Maxwell’s equations for an unconnected collection of scatterers,” Ph.D. Thesis, University of Toulouse 3, France, 2006.
  13. Mouysset, V., P. A. Mazet, and P. Borderies, “A new approach to evaluate accurately and efficiently electromagnetic fields outside a bounded zone with time-domain volumic methods,” *Journal of Electromagnetic Waves and Applications*, Vol. 20, 803–817, 2006.
  14. Olivier, J. C., “On the synthesis of exact free space absorbing boundary conditions for the finite-difference time-domain method,” *IEEE Trans. on Ant. and Prop.*, Vol. 40, 456–460, 1992.
  15. Rubio Breto, A. and A. Monorchio, “Time-domain hybrid methods to solve complex electromagnetic problems,” *EMC Congress*, Istanbul, 2003.
  16. Al Sharkawy, M. H., V. Demir, and A. Z. Elsherbeni, “The iterative multi-region algorithm using a hybrid finite difference frequency domain and method of moment techniques,” *Progress In Electromagnetics Research*, PIER 57, 19–32, 2006.
  17. Shlager, K. L. and G. S. Smith, “Near-field to near-field transformation for use with the FDTD method and its application with pulsed antenna problems,” *Electronics Letters*, Vol. 30, 1262–1264, 1994.
  18. Shlager, K. L. and G. S. Smith, “Comparison of two FDTD near-field to near-field transformations applied to pulsed antenna problems,” *Electronics Letters*, Vol. 31, 410–413, 1995.
  19. Wang, S. G., X. P. Guan, D. W. Wang, X. Y. Ma, and Y. Su, “Electromagnetic scattering by mixed conducting/dielectric objects using higher-order MOM,” *Progress In Electromagnetics*

- Research*, PIER 66, 51–63, 2006.
20. Xu, F. and W. Hong, “Analysis of two dimensions sparse multicylinder scattering problem using DD-FDTD method,” *IEEE Trans. on Ant. and Prop.*, Vol. 52, 2612–2617, 2004.
  21. Yee, K. S., “Numerical solution of initial boundary value problems involving Maxwell’s equations in isotropic media,” *IEEE Trans. on Ant. and Prop.*, Vol. 14, 302–307, 1966.
  22. Yee, K. S., “Time-domain extrapolation to the far field based on FDTD calculations,” *IEEE Trans. on Ant. and Prop.*, Vol. 39, 410–413, 1991.